Interphase chromosomes undergo constrained diffusional motion in living cells

W.F. Marshall*||, A. Straight†, J.F. Marko‡, J. Swedlow§, A. Dernburg*°, A. Belmont¶, A.W. Murray†, D.A. Agard¥* and J.W. Sedat*

Background: Structural studies of fixed cells have revealed that interphase chromosomes are highly organized into specific arrangements in the nucleus, and have led to a picture of the nucleus as a static structure with immobile chromosomes held in fixed positions, an impression apparently confirmed by recent photobleaching studies. Functional studies of chromosome behavior, however, suggest that many essential processes, such as recombination, require interphase chromosomes to move around within the nucleus.

Results: To reconcile these contradictory views, we exploited methods for tagging specific chromosome sites in living cells of *Saccharomyces cerevisiae* with green fluorescent protein and in *Drosophila melanogaster* with fluorescently labeled topoisomerase II. Combining these techniques with submicrometer single-particle tracking, we directly measured the motion of interphase chromatin, at high resolution and in three dimensions. We found that chromatin does indeed undergo significant diffusive motion within the nucleus, but this motion is constrained such that a given chromatin segment is free to move within only a limited subregion of the nucleus. Chromatin diffusion was found to be insensitive to metabolic inhibitors, suggesting that it results from classical Brownian motion rather than from active motility. Nocodazole greatly reduced chromatin confinement, suggesting a role for the cytoskeleton in the maintenance of nuclear architecture.

Conclusions: We conclude that chromatin is free to undergo substantial Brownian motion, but that a given chromatin segment is confined to a subregion of the nucleus. This constrained diffusion is consistent with a highly defined nuclear architecture, but also allows enough motion for processes requiring chromosome motility to take place. These results lead to a model for the regulation of chromosome interactions by nuclear architecture.

Addresses: Departments of *Biochemistry and Biophysics, †Physiology, §Cellular and Molecular Pharmacology, University of California at San Francisco, San Francisco, California 94143, USA. ‡Department of Physics MC273, University of Illinois at Chicago, Chicago, Illinois 60607-7059, USA. ¶Department of Cell and Structural Biology, University of Illinois, Urbana-Champaign, Urbana, Illinois 61801, USA. ¥Howard Hughes Medical Institute, University of California at San Francisco, San Francisco, California 94143, USA.

Present addresses: ||Department of Biology, Yale University, New Haven, Connecticut 06520, USA. °Department of Developmental Biology, Stanford University, Palo Alto, California 94305, USA.

Correspondence: J.W. Sedat
E-mail: sedat@msg.ucsf.edu

Received: 1 September 1997
Revised: 16 October 1997
Accepted: 16 October 1997

Published: 5 November 1997

Current Biology 1997, 7:930–939
http://biomednet.com/elecref/0960982200700930

Background

Structural studies of the nucleus demonstrate conclusively that chromosomes are not scattered randomly in the nucleus but are, in fact, arranged in a highly defined nuclear architecture. Particular loci are found reproducibly at specific nuclear locations [1], suggesting that the nucleus is a static structure, with chromosomes held rigidly in place by some sort of nuclear skeleton or matrix. Consistent with this view, a recent study using fluorescence recovery after photobleaching (FRAP) indicated that interphase chromatin appears to be essentially immobile at spatial scales greater than 0.4μm [2]. Experiments in which nuclei were irradiated with an ultraviolet microbeam and the subsequent position of the damaged DNA was imaged after various time intervals [3], also indicated that chromatin did not drift extensively. Furthermore, visualization of chromatin in living cells by time-lapse microscopy does not, in general, reveal any large, visually obvious, chromatin displacements [4–6]. Thus, both FRAP analysis and direct visualization appear to confirm the suspicion that chromatin may be effectively immobile inside the nucleus.

The picture of the nucleus as a static structure, containing immobile chromatin held in precise positions, contrasts strongly with the more dynamic view of chromatin suggested from its behavior. Indeed, movement of chromatin underlies many essential biological processes including meiotic homolog pairing, recombination, enhancer looping and chromosome condensation. We are thus faced with an apparent contradiction — chromatin is organized into fixed positions within the nucleus, but it can also move around inside the nucleus to interact with other regions of chromatin. This raises the possibility that chromatin may actually be mobile, but that the displacements are too small for FRAP analysis or direct microscopic visualization to detect.

In this report we attempt to resolve this issue by direct and quantitative tracking of the movement of specific

chromosome regions in real time in living cells of *Saccharomyces cerevisiae* and *Drosophila melanogaster*. Our method involves labeling yeast chromosomes with green fluorescent protein [7,8] or *Drosophila* chromosomes with microinjected fluorescent topoisomerase II [9], along with three-dimensional submicrometer single-particle tracking to analyze the motion [10,11]. We demonstrate that chromatin does indeed undergo diffusive random walk motion within the nucleus, with a diffusion constant large enough to account for the kinetics of motion-requiring nuclear processes. This diffusive motion is, however, constrained such that although chromatin can diffuse freely over sufficiently small spatial scales, a given chromosome region is confined to a small subregion of the nucleus. This constrained diffusional motion thus reconciles the dynamic behavior of chromatin inferred from functional studies with the high degree of positional specificity indicated by structural studies.

We consider next the physical basis for the observed motion. This is especially important when attempting to understand the mechanism and kinetics of processes, such as recombination, which require chromatin motion. Is the passive diffusion of chromatin by Brownian motion sufficiently fast to account for these processes, or is active motility required to move chromatin from one place to another? The importance of motor-protein-driven motility in movements of mitotic chromosomes and of cytoplasmic components, such as vesicles and mitochondria, is well established. The use of active motility to circumvent the slow diffusion of large cellular structures is also likely to be widespread. This issue was first raised for nonmitotic chromosomes by McClintock [12] who pointed out that the chromosome rearrangements seen during the pairing of meiotic homologs might require special motile machinery to pull the chromosomes together, but could potentially also take place by random diffusion. The large size of the chromatin polymer, and the density with which it is packed into the nucleus, suggest that chromatin would diffuse extremely slowly by Brownian motion [13], leading to the proposal of more active mechanisms for chromosome movements during homolog pairing [14]. Similarly, for any process that requires movement of chromatin over significant distances in the nucleus, we must ask whether it could occur by diffusion alone. In this report, we demonstrate that chromatin motion continues in the absence of active metabolism, which implies that the motion is due to Brownian motion and not to active motility. Finally, we demonstrate that chromatin confinement is microtubule-dependent, a surprising result that suggests a possible role for the cytoskeleton in the maintenance of nuclear architecture.

Results

Measuring diffusional motion of chromatin by sub-micrometer single-particle tracking

To track chromatin in the yeast *S. cerevisiae*, we visualized arrays of *lac* operator sites inserted in the yeast genome, by expressing a construct encoding the Lac repressor protein fused to green fluorescent protein (GFP) [7,8]. Diploid yeast cells homozygous for an insertion of the *lac* operator array into the *LEU2* locus near the centromere of chromosome III were imaged in three dimensions as shown in Figure 1. Only unbudded (G1 phase of the cell cycle) cells were examined. Cells survived imaging as judged by their ability to subsequently undergo successful mitotic nuclear division. Once the position of the *lac* operator array has been imaged over time, its diffusion constant can be computed. Determination of a diffusion constant from time-lapse images of an object is a well established technique known as submicrometer single-particle tracking [10,11],

Figure 1

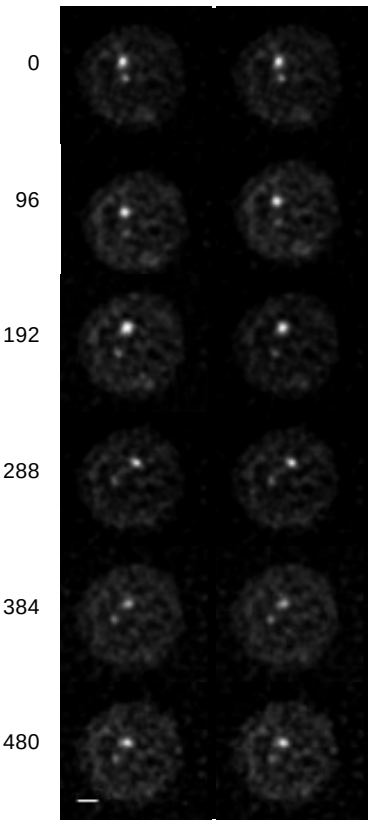

Visualizing interphase chromatin motion in living yeast cells in three dimensions. Stereo pairs show successive time-lapse three-dimensional images of a diploid yeast cell homozygous for an insertion of a *lac* operator array at the *LEU2* locus and expressing a GFP–Lac repressor fusion protein [7]. Relative motion of the two homologous loci *in vivo* is clearly evident. Yeast cells imaged under these conditions remain viable as judged by their ability to bud and undergo mitotic divisions successfully. Note that the large round object seen dimly in the background is the whole cell, not the nucleus, and the background staining represents GFP–LacI molecules in the cytoplasm. Elapsed time since the beginning of the experiment is given in seconds to the left of each image. Scale bar = 1 μm.

and relies on the fact that, by locating the center of mass of the object in an image, submicrometer displacements much smaller than the resolution limit of the microscope [10] can be measured with a precision limited only by the signal-to-noise ratio of the image.

At each time point, the three-dimensional distance, $d(t)$, between the two GFP spots was measured. We measured distance between two spots, rather than the position of a single spot, in order to compensate for possible drift or rotation of the nucleus [4,5] which might otherwise lead to apparent motion. A plot of $d(t)$ for one nucleus is given in Figure 2a. As the two sites diffuse towards and away from each other, the distance between them will increase and decrease at random. Over very short time intervals, the change in distance will generally be small, whereas over longer time intervals each site will have diffused more and, hence, the magnitude of the change will be greater on average. The average change in distance will thus increase with increase in time interval [11]. From the relationship between the average change in distance and the length of the time interval, we computed the diffusion constant. Denoting a time interval by Δt and the change in distance d during this interval by Δd, we computed the mean squared change in $d(t)$ as $\langle \Delta d^2 \rangle = \langle [d(t) - d(t + \Delta t)]^2 \rangle$. For two particles undergoing three-dimensional random walks with diffusion constant D, it can be shown that a plot of $\langle \Delta d^2 \rangle$ against Δt should increase linearly [15] with a slope of 4D. A total of 110 data records, each from a different cell, were averaged and plotted in Figure 2b. Over short time intervals, we observed a monotonic increase of $\langle \Delta d^2 \rangle$ with increasing Δt, suggesting diffusive motion [11]. Directional linear motion, such as that produced by motor proteins translocating on microtubules, would lead to an upwardly curving parabolic curve for Figure 2b [11], but this was not evident in our data. Hence we conclude that the chromatin motion seen is a random walk diffusive motion rather than a type of directed motility.

For long time intervals, in contrast, the plot in Figure 2b is horizontal, implying that the average displacement is independent of the time interval. This long-time-scale behavior implies that the diffusion of the two particles is constrained [11]: each particle is confined to diffuse within a limited region from which it cannot escape. Such confinement could occur if the chromatin was tethered to the nuclear envelope or some internal nuclear skeleton. The plateau height reflects the size of the confinement region,

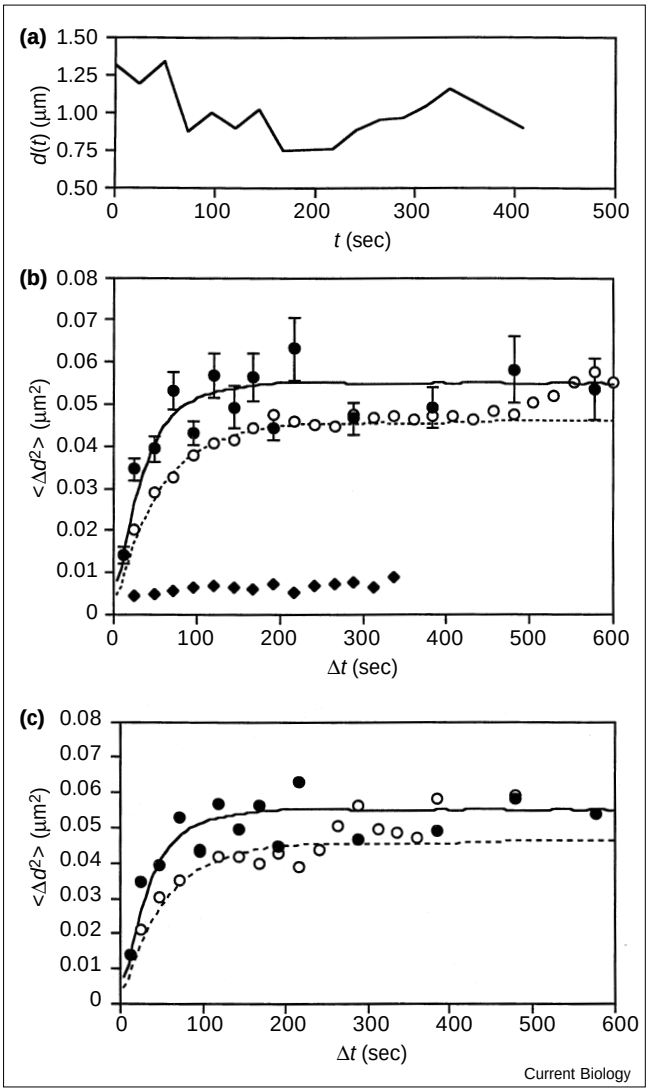

Figure 2

Constrained diffusion of chromatin in living yeast cells. (a) Typical data record obtained by submicrometer single-particle tracking, showing a plot of the distance between GFP spots $d(t)$ against time t. In such traces, the distance between spots decreases and increases at random as the two spots diffuse toward and away from each other. (b) Overall mean-squared change in distance between GFP spots $\langle \Delta d^2 \rangle$ plotted against elapsed time interval Δt between distance measurements. Solid circles represent living yeast cells; a total of 110 data records, each containing an average of 13 time points, were combined in this plot. Note that although (a) demonstrates that the distance between spots both increases and decreases randomly, the mean-squared change in distance always increases with increasing time interval [11] – the longer the time interval between measurements, the more the distance between two diffusing points is expected to change. For long time intervals, $\langle \Delta d^2 \rangle$ becomes independent of Δt and the plot reaches a plateau, indicating a constraint on diffusion. The solid line is the best-fit curve derived by computer simulation using parameters $D = 5 \times 10^{-12}$ cm^2/sec and confinement radius $R = 0.3\,\mu$m for data from live yeast cells. Solid diamonds, yeast cells fixed in 3.7% formaldehyde imaged under identical conditions. Motion in living cells is much greater than in fixed cells, and is thus not due merely to measurement error. Open circles, chromatin motion in azide-treated yeast cells showing only slightly reduced motion relative to living cells. The broken line is the best-fit curve derived using $D = 3 \times 10^{-12}$ cm^2/sec and $R = 0.25\,\mu$m for data from azide-treated cells. (c) Chromosome diffusion is independent of size: diffusion of a small *CEN* plasmid compared to that of a chromosome. Solid circles, motion of the centromere of chromosome III (reproduced from panel (b) for comparison). Open circles, motion of *CEN* plasmid. The broken line is the best-fit curve derived by computer simulation using $D = 3 \times 10^{-12}$ cm^2/sec, $R = 0.25\,\mu$m.

while the steepness of the plot at shorter time scales depends on the diffusion constant [11]. Computer simulations of constrained diffusion were used quantitatively to relate the slope and plateau height observed in Figure 2b with the diffusion constant (D) and confinement radius (R) of the constrained diffusion model. On the basis of such simulations, we find the data are best described by a particle with $D = 5\times10^{-12}\,cm^2/sec$ confined to a region of radius $R = 0.3\,\mu m$ (root mean square fitting error in $\langle\Delta d^2\rangle$ is $4\times10^{-3}\,\mu m^2$). This radius is significantly smaller than the radius of the diploid nucleus (about 1.5μm), and thus reflects confinement of the chromatin to a small nuclear subregion, about one percent of the volume of the nucleus.

Experimental resolution and precision are sufficient for reliable measurement of chromatin motion

The optical resolution and measurement precision of our experiments were found to be sufficient to measure chromatin motion reliably. Precision is of particular concern because random error in the position measurements — due, for example, to noise in the image or mechanical jitter in the microscope — would generate data resembling a constrained random walk. To rule out this possibility, we measured the apparent motion in formaldehyde-fixed cells under identical conditions. Intensities, and hence the signal-to-noise ratios, were the same as for live cells, leading to equivalent measurement precision. Any motion seen in fixed cells is due, at least in part, to limited measurement precision. Motion in fixed cells thus provides an upper limit on the apparent motion attributable to measurement error. If the apparent motion was due only to errors in position measurement, then the data from fixed cells should closely resemble the data from live cells. As plotted in Figure 2b, motion in living cells was in fact much greater than in fixed cells, and thus cannot be due simply to limited measurement precision. Using data from fixed cells, position measurement error was estimated to be less than 0.04 μm (see Materials and methods), which is small relative to the displacements recorded in living cells. We conclude that measurement errors are insignificant compared to the actual displacements of the chromatin.

Evaluating alternative models for observed displacements

We have so far presumed that the changes in distance between labeled sites result from chromatin diffusion. Several alternative explanations exist, however, and so must be ruled out. The most obvious possibility is nuclear rotation [4,5]. If a single focal plane through a cell is observed, the apparent distance between two spots can appear to change due to rotation or rocking of the nucleus, without any actual change in distance between the spots. This is because a two-dimensional distance measurement only measures distance in projection, and depends on the angle of the projection. To avoid this possibility, all measurements were carried out in three dimensions using optical sectioning microscopy. The three-dimensional distance measurement is unaffected by rotation of the nucleus and thus provides a more reliable indication of distance. We can thus immediately rule out nuclear rotation as a cause of the apparent diffusive motion.

Another possible cause of displacement could be forces exerted on the sample by pressure from the microscope objective lens. This is of particular concern in three-dimensional microscopy because the stage is rapidly moving up and down. To rule out this possibility, identical measurements were made in two dimensions by acquiring a series of images at a fixed focal plane in living cells without moving the objective or sample; forces exerted on the sample by the objective lens can thus be eliminated. The magnitude of the displacements observed in these two-dimensional experiments is comparable to that seen in the three-dimensional measurements (data not shown), and is similarly eliminated when the cells are fixed. We conclude that the displacements we observe are not simply a consequence of pressure from the objective lens on the coverslip.

The constrained motion observed here could, in principle, be explained if the chromatin was fixed within a nucleus that was itself undergoing elastic deformations. These deformations would cause proportional displacements between any pair of points embedded in the nucleus, and would give rise to an apparent constraint if the deformations were limited in extent. This model predicts that the displacement between two points resulting from an elastic deformation of the entire nucleus will be proportional to the distance between the points. However, when the average magnitude of the displacements $\langle|d(t)-d(t+\Delta t)|\rangle$ was plotted against the distance $d(t)$, for a fixed time interval $\Delta t = 24$ seconds, no such correlation was seen (data not shown). Hence, the observed motions are unlikely to result from a simple elastic deformation.

Chromatin motion does not require active metabolism

What is the physical basis of chromatin motion? The random walk motion could be due either to Brownian motion, involving collisions with thermally excited solvent particles, or else it could be driven by enzymes or motor proteins. The answer is not obvious because, in addition to the enzymes of DNA metabolism which can act as force-producing motors [16], the nucleus contains a number of potential ATPases, such as the structural maintenance of chromosomes (SMC) family of proteins [17,18], thought to produce conformational changes (and hence motion) in chromatin. Conventional motor proteins, including myosin/actin-related proteins [19,20] have also been identified in the nucleus. If interphase chromatin motion is due to the action of such mechanoenzymes, active metabolism would be required to support the movements. To test a requirement for metabolic activity, we repeated

Figure 3

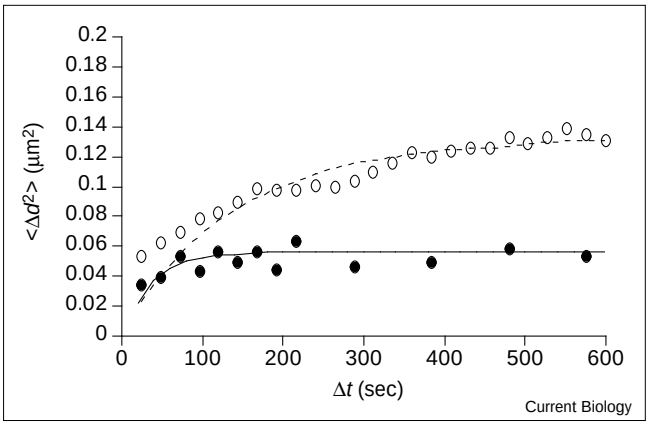

Confinement of chromatin is dependent on microtubules. Open circles, motion in cells treated with 15 μg/ml nocodazole in YPD medium. Closed circles, untreated cells. Solid line, best-fit curve derived by computer simulation using $D = 5\times10^{-12}$ cm²/sec, R = 0.3 μm for the untreated cells. Broken line, best-fit curve using $D = 3\times10^{-12}$ cm²/sec, R = 0.7 μm for the nocodazole data. In the presence of nocodazole, the confinement radius shifts from 0.3 μm, corresponding to a volume of 0.11 μm³, to 0.7 μm, corresponding to a volume of 1.4 μm³, which represents a 10-fold expansion of the confinement region.

the motion measurement following incubation in, and in the continued presence of, 0.02% azide, which poisons cellular metabolism by blocking the respiratory electron transport chain. This concentration of azide is lethal and immediately arrests cell division and mitotic chromosome movements (data not shown) as well as other types of intracellular motility in yeast [21]. As illustrated in Figure 2b, diffusion of chromatin is only slightly reduced in the presence of this lethal dose of azide. Because chromatin motion continues in the absence of active metabolism, it is likely that it reflects true Brownian motion.

Chromatin diffusion is independent of chromosome size

Diffusional mobility generally depends on the size of the diffusing object. If chromatin motion depends on chromosome size, large and small chromosomes or plasmids would differ in their ability to move around in the nucleus, and hence in their ability to participate in interactions like recombination that require motion. A dependence of chromosome mobility on size is very much to be expected. The diffusion of tracer molecules in the cytoplasm depends strongly on the size of the molecules [22]. To determine how a chromosome's size affects its diffusional mobility in the nucleus, we measured the motion of a small circular centromere-containing plasmid. We used a 15 kilobase (kb) plasmid containing a centromere sequence (*CEN*); 10 kb of the plasmid was *lac* operator repeats and thus most of the plasmid could be visualized. Cells carrying two copies of the plasmid and thus showing two distinct spots of fluorescence were used to compute $\langle\Delta d^2\rangle$ against Δt (Figure 2c). We expected that the plasmid, being much smaller than a chromosome, should have a much higher diffusion constant. Surprisingly, the diffusion constant for the plasmid was 3×10^{-12} cm²/second, slightly less than that for a chromosome. Thus, contrary to expectation, loci on shorter pieces of chromatin do not necessarily diffuse faster than loci on longer ones. But plasmid chromatin was found to be confined just like an entire chromosome. If confinement of diffusion in fact reflects tethering of discrete chromosome sites to an immobile structure, then the diffusion constant would depend not on the overall size of the chromosome but only on the length of chromatin between successive tethering points.

Confinement of diffusion is microtubule-dependent

Constrained diffusion suggests that chromatin is tethered to an immobile structure, but the identity of this structure is unknown. To test whether microtubules play a role in confining chromatin, we treated yeast cells with nocodazole. As seen in Figure 3, when microtubules were depolymerized with nocodazole, chromatin diffusion was much less confined, and there was an expansion of the confinement region. This surprising result suggests that microtubules play a role in chromatin confinement, either through a direct interaction between interphase chromatin and intranuclear microtubules or more indirectly through an interaction of nuclear structures with cytoplasmic microtubules. Microtubules are not generally thought to be present in interphase nuclei, although intranuclear microtubules have been observed in interphase in some fungi [23]. In either case, the fact that chromatin confinement can be removed or reduced by pharmacological treatment verifies the existence of actual confinement by demonstrating that the chromatin has the capacity for unconfined motion.

Drosophila chromatin also undergoes constrained diffusion

To ascertain the generality of the phenomenon of constrained diffusion of chromatin, we measured chromatin motion in *D. melanogaster* by exploiting the specific localization pattern of topoisomerase II. In *Drosophila*, topoisomerase II accumulates primarily at one or two discrete foci per nucleus [9]. To test whether these foci reflect site-specific chromosome binding, immunofluorescence was carried out in *Drosophila* embryos [24] using anti-topoisomerase II antibodies, following fluorescence *in situ* hybridization (FISH) using DNA probes to heterochromatic satellite regions [25]. The topoisomerase II spot did not coincide with the rDNA locus or the Responder of segregation distorter (Rsp) heterochromatin block, but co-localized precisely with the 359 base pair (bp) repeat block [26,27] on the X chromosome (Figure 4). The positions and shapes of the FISH and immunofluorescence signals exactly coincide, implying that topoisomerase II binding is

Figure 4

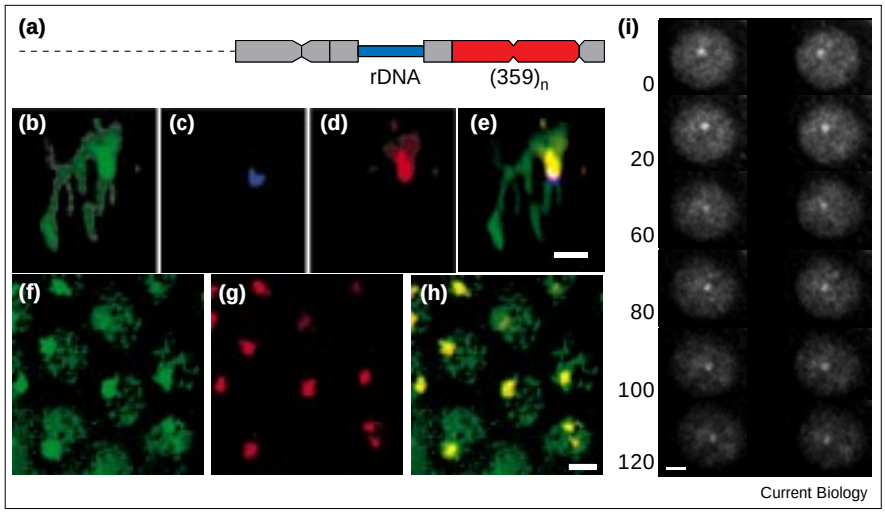

Visualizing interphase chromatin motion in *Drosophila*. Topoisomerase II binds at the 359 bp repeat region on the X chromosome in *Drosophila* embryos. (a) Heterochromatin of the X chromosome [27]. (b–e) Simultaneous fluorescent *in situ* hybridization (FISH) and immunofluorescence demonstrating topoisomerase II accumulation at the 359 bp repeat in anaphase. (b) Anti-topoisomerase II immunofluorescence. (c) FISH using a probe to the rDNA locus (d) FISH using probe to the 359 bp repeat. (e) overlay of (b), (c) and (d). Clearly, the topoisomerase II signal completely coincides with the 359 bp signal but not with the neighboring rDNA. Bar = 2.0 μm. (f–h) Topoisomerase II localization in interphase. (f) anti-topoisomerase II immunofluorescence. (g) FISH using a probe to the 359 bp repeat. (h) Overlay showing complete coincidence of the two signals. Bar = 2.0 μm. (i) Injection of rhodamine-labeled topoisomerase II allows visualization of the 359 bp repeat region *in vivo* in three dimensions. Times corresponding to each stereo pair are given in seconds. Bar = 2.0 μm. Embryos imaged under these conditions remain viable: after imaging, embryos were maintained in humidified chambers until hatching. Embryos that were imaged hatched with the same frequency as embryos injected with buffer and not imaged. During imaging, synchronized mitoses occurred on schedule and no chromosome segregation defects such as anaphase bridges were observed.

co-extensive with the entire 359 bp repeat region. In agreement with these findings, the most common topoisomerase II-specific drug-stimulated cleavage site in the *Drosophila* genome is found in the 359 bp repeat sequence [28]. Thus, topoisomerase II is one of a growing number of proteins known to bind to specific heterochromatic regions [29,30]. This localization provides a means of tracking a specific chromosome region: by injecting fluorescently labeled topoisomerase II into living embryos [9] the foci of topoisomerase II accumulation can be imaged, revealing the motion of the underlying chromatin (Figure 4i). Embryos remained alive during imaging as judged by the occurrence of normal synchronized nuclear divisions and subsequent successful hatching.

To compensate for nuclear drift, we computed the distance $r(t)$ from the topoisomerase II spot to the center of the nucleus (Figure 5a). For a particle with diffusion constant D, a plot of $\langle \Delta r^2 \rangle$ against Δt should be linear with slope 2D. Just as in the case of two diffusing particles, confinement will cause the plot to reach a plateau at large time intervals. We plotted $\langle \Delta r^2 \rangle$ against Δt for 27 nuclei from six different *Drosophila* embryos (Figure 5b). The data are best fit by simulations of a diffusing particle with a diffusion constant $D = 2.0 \times 10^{-11}$ cm^2/sec, a slightly larger value than in yeast, and a confinement radius of 0.9 μm. This confinement is interesting because the 359 bp repeat is a scaffold-associated region (SAR) in *Drosophila* [28], and may thus reflect the attachment of chromatin to an internal nuclear skeleton [31].

Discussion

Comparison with other studies of chromatin motion

Previous studies of chromatin in living cells using time-lapse microscopy have generally indicated that rotational motion of the nucleus is the predominant type of chromatin motion [4,5]. Our study differs from these studies in that we have deliberately chosen to use rotationally invariant measures (d and r), so that changes of position within the nucleus, rather than overall nuclear rotation, can be measured directly. Apart from nuclear rotation [4,5], apparent Brownian motion of chromosomes within the nucleus has not been reported previously. The small diffusion constants measured here, together with the finding that chromatin diffusion is constrained, makes the diffusive motion unlikely to be noticed unless explicitly tested for, using the type of analysis employed here.

A recent study has used FRAP to measure chromatin diffusion in cells in culture [2]. Nuclei labeled with an intercalating DNA stain were photobleached by a laser beam focused to a spot of 0.8 μm diameter and, after bleaching, the time-course of recovery of fluorescence was measured. Because the recovery of fluorescence was incomplete, it was concluded that chromatin was not mobile. Our approach of directly tracking chromatin motion, with the finding that chromatin undergoes confined diffusion, allows us to suggest a different interpretation for the FRAP data. Chromatin diffusion is confined to spatial scales less than 0.3 μm (the size of the confinement region), a conclusion also reached by FRAP. On smaller

Figure 5

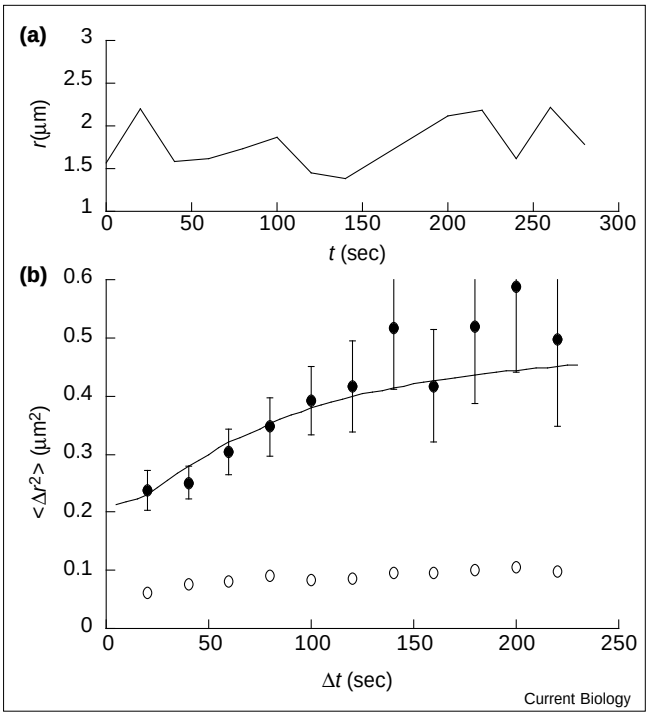

Chromatin diffusion in *Drosophila.* (a) plot of distance *r* from the center of the nucleus to the topoisomerase II spot, over time, for a single nucleus. (b) Mean-squared change in distance plotted against time interval. Solid circles, data from living embryos. A total of 27 data records, each containing an average of nine time points, were combined in this plot. Solid line, the best-fit simulation result corresponding to $D = 2.0\times10^{-11}$ cm²/sec and R = 0.9 μm. Open circles, fixed embryos stained with anti-topoisomerase II antibodies and imaged under identical conditions.

scales — inaccessible to FRAP because of the relatively large size of the bleached spot but measurable by our direct tracking approach — the chromatin is in fact fully capable of diffusional motion, as required for the dynamic functional behavior of chromatin.

Comparison of chromatin diffusion with the diffusion of other biopolymers

Chromatin moves with a diffusion constant much lower than that previously reported for biological macromolecules. Proteins have diffusion constants around 10^{-6} cm²/second in aqueous solution and 10^{-8} to 10^{-7} cm²/sec in cytoplasm [32]. The slower diffusion of chromatin is not surprising given the extremely large size of an interphase chromosome. Chromatin also diffuses more slowly than DNA in dilute solution, which has a diffusion constant ranging from 10^{-8} to 10^{-9} cm²/sec for DNA that is 4 to 300 kb in length [33]. The high concentration of chromatin within the nucleus would predict that chromatin *in situ* should have more difficulty diffusing than does DNA in dilute solution.

Comparison of chromatin diffusion with predictions from theoretical polymer dynamics

We next compare the diffusion constant of chromatin with that expected for a large polymer in free solution [34] in which $D_{free} = 0.2\,kT/\eta R$ where $kT = 4\times10^{-14}$ erg at room temperature, η is viscosity, and R is average end-to-end polymer length. For the CEN plasmid, an approximation for R is the radius of the GFP signal, which is less than 0.5 μm: this upper limit on R provides a lower limit for D_{free}. Nucleoplasm viscosity is in the range 1.0–10.0 cP [35,36]. A value of $\eta = 5$ cP gives a minimum D value of 3×10^{-9} cm²/sec, which is three orders of magnitude larger than the experimental value. This discrepancy is difficult to reduce with reasonable changes in R or in η. But chromatin is not in dilute solution. As with other macromolecules [22], crowding and entanglement will impede chromatin motion. We can estimate these effects on the basis of the theory of reptation [37], assuming that chromatin is a random polymer [38] entangled with itself and with other chromatin polymers. The entanglements delimit a tube within which the polymer diffuses with diffusion constant D_t. The n entanglement sites per chain divide it into n subchains, each with average radius $R_{sub} = R/(n^{1/2})$, so each subchain has diffusion constant $D_{free}n^{1/2}$. A string of n subchains thus diffuses through the tube with diffusion constant $D_t \sim (1/n)D_{free}n^{1/2} = D_{free}/n^{1/2}$. The time τ^* to diffuse out of the tube is $\tau^* = L^2/D_t$ where the tube contour length is $L = nR_{sub}$. Simultaneously, the center of mass of the polymer diffuses a distance R. Hence, $D_{entangled} \sim R^2/\tau^* = R^2D_t/L^2 = D_t/n$ (since $L^2 = nR^2$), so the final diffusion constant $D_{entangled} = D_{free}/n^{3/2}$. A modest number ($n$~20) of entanglements would reduce the diffusion constant by two orders of magnitude. The observed D value is thus consistent with Brownian motion of an entangled polymer.

Diffusion-driven mechanisms for processes that require chromosome motion

Many essential processes require interphase chromosomes to move over significant distances within the nucleus. Examples include meiotic homolog pairing, somatic recombination and chromosome condensation. In imagining possible mechanisms for these processes, we consider two general classes: diffusion-driven mechanisms and mechanisms that rely on active motility. A well-known example of the latter is mitosis, in which a microtubule-based motility system is used first to drive chromosomes to the metaphase plate and then to segregate them to the spindle poles. Other processes, such as homolog pairing or recombination, which involve chromosome movements of a comparable magnitude, may also depend on active mechanisms.

The alternative to active motility is a diffusion-driven mechanism that would require two chromatin sites to be driven by thermal motion until they collide at random and

then interact. Most protein–protein or protein–DNA interactions are diffusion-driven but, as noted above, the diffusion constants for proteins, even in the crowded conditions of living cytoplasm, are generally high enough for diffusion-driven mechanisms to be effective. We are thus left with a straightforward quantitative question: is chromatin diffusion sufficiently fast to be effective, or given the small chromatin diffusion constant, is some other active mechanism operating? A process such as recombination might entail chromatin movements of several micrometers. Given a diffusion constant in the range 10^{-12} to 10^{-11} cm^2/sec, it would take roughly one to ten minutes for chromatin to diffuse 1 μm, which is sufficiently fast compared to the duration of interphase (greater than one hour). We conclude that diffusion-driven mechanisms for processes requiring chromatin motion are compatible with the measured rate of chromatin diffusion.

Confinement of diffusion

Constrained diffusion has important implications for nuclear processes involving motion. For two loci to interact, their confinement regions must overlap, or else the interaction will be prevented because the loci will never be sufficiently close. On the other hand, if the confinement regions of two loci do overlap, the frequency of collisions between the loci will actually be higher than if the loci were unconfined, because they will be forced to remain in the same general vicinity. Thus, as a result of constrained diffusion, nuclear architecture, which fixes the positions of loci in the nucleus, becomes a dominating factor in determining whether a particular interaction can or cannot occur. A picture thus emerges of interphase chromatin being able to diffuse within the nucleus, but only to a limited extent. This result is consistent with our recent studies of nuclear positioning during interphase in *Drosophila*, which indicated that, for 42 different loci examined, each was consistently found in approximately the same locus-specific position in all nuclei [39].

The alleviation of confinement by nocodazole suggests that microtubules play some role in chromatin confinement. We note however that in yeast, the tagged site is near a centromere, and if confinement reflects a direct interaction of the centromere with interphase microtubules that are nucleated by the spindle pole body, this could explain the effect of nocodazole treatment. Microtubule-dependent confinement could thus be a consequence of the closed mitosis of yeast, in which the spindle pole body remains embedded in the nuclear envelope. It is unclear whether this microtubule dependence will be a general feature of chromatin motion in other cell types.

Although confinement may reflect physical interaction with the nuclear envelope, spindle pole body or nuclear matrix, it may simply reflect the limited interstitial space between chromatin fibers. We can apply Ogston's [40] formula to determine the average void space in a solution of random fibers, $\langle R \rangle = (4L)^{-1/2}$ where L is the average chain density. Given a contour length of 75 μm if the 25 megabase diploid yeast genome is packed as a 30 nm fiber, and given a nuclear radius 1.5 μm, we get $L = 5\ \mu m^{-2}$. Thus, the average gap $\langle R \rangle$ between fibers is 0.2 μm and is similar to the observed confinement radius. The exact nature of the confinement is thus unclear and could reflect either tethering to a structure or crowding by neighboring chromatin chains. This question will be the subject of future experiments.

Measurement of physical properties from motion in living cells

Many processes in cell biology, such as chromosome segregation or intracellular transport of vesicles and organelles, are essentially mechanical. In such cases, the mechanical properties of the relevant cellular structures are of fundamental importance. Direct measurement of properties such as rigidity, viscosity or diffusional mobility could, in principle, be made using isolated cellular components *in vitro*, but the cellular environment is likely to strongly influence the physical behavior of such large-scale structures. This is particularly true of chromatin, the conformation of which is notoriously sensitive to the buffer conditions used for isolation. Clearly, an ideal approach would be to make mechanical measurements inside the living cell using minimally invasive means. Physical manipulation within living cells using microneedles [41] or laser tweezers [42] has proven an invaluable tool for understanding chromosome motion during mitosis, but in situations in which the cellular structures are too small, too delicate, too densely packed or otherwise inaccessible to micromanipulation procedures, an approach based on pure observation is highly desirable. As illustrated by the present study, three-dimensional time-resolved visualization of movements of cellular structures in living cells, when coupled with quantitative motion analysis, provides a powerful tool for measuring mechanical behavior while minimizing perturbation of the cell. This approach of inferring mechanistic behavior from analysis of motion, which has played an exceedingly important role in physics and astronomy, should, with the advent of routine three-dimensional microscopy and quantitative motion analysis, be applicable to a broad range of problems in cell biology.

Conclusions

Our primary conclusion is that interphase chromatin undergoes constrained Brownian motion. A segment of chromatin is confined within a small subregion of the nucleus, representing roughly one percent of the nuclear volume, and cannot move out of this region of confinement; but within this region, the chromatin segment undergoes diffusive motion with a diffusion constant in the range 10^{-12} to 10^{-11} cm^2/sec. The simplest model is

that this confinement reflects the attachment of chromatin to an immobile superstructure in the nucleus, which then confines the segment of chromatin between successive attachment points. A series of such attachment points distributed along a chromosome—for example, the set of nuclear envelope association sites present in *Drosophila* [39]—would thus partition the chromosome into a set of domains [43,44], each reflecting a confinement region. This model has important implications for our understanding of processes involving chromatin motion, such as recombination or homology searching. As long as the confinement regions for two chromosome segments are overlapping, Brownian motion of the chromatin within those regions will be fast enough to allow a diffusion-driven interaction between them to take place on a reasonable time scale. If the two confinement regions do not overlap, however, then an interaction between the two chromosome segments will be effectively prevented. Constrained diffusion therefore provides a mechanism by which nuclear architecture exerts a kinetic control over chromosome interactions.

Materials and methods

In vivo *imaging of chromatin motion in* S. cerevisiae

Cells were grown and mounted as described [7]; such cells grow and divide normally. Time-lapse three-dimensional images were collected at rates of one three-dimensional data set every 12 sec, 24 sec or 96 sec, by wide-field deconvolution three-dimensional microscopy [45] using a 60× N.A. 1.4 objective and 1.5180 oil. At each time point, fourteen 256×256 pixel images were collected at focal plane increments of 0.25 μm per plane.

Simulation of constrained random walk motion

Random walks were simulated on a cubic lattice [46] for two particles. Every time step ($\tau = 50$ msec), x, y and z coordinates of the particle were independently increased or decreased (with equal probability) by $\delta = 2D\tau$. To represent confinement, steps causing a particle to exceed a confinement distance of R from its initial position were rejected, and a new step chosen. The distance $d(t)$ between the two particles was stored every 5 sec of simulation, with 1800 steps stored per run. Finally, 200 runs were averaged to compute a plot of $\langle \Delta d^2 \rangle$ against Δt. Simulations were run for different values of D and R, changing D in increments of 0.5×10^{-12} cm^2/sec and R in 0.025 μm increments. For each set of values, observed data and the simulation were compared, and the D and R values resulting in the least squared error were chosen. For *Drosophila* data, simulations were carried out using only a single diffusing particle and taking distance from a fixed reference point.

Estimation of distance measurement error

We approximate the observed distance $d(t)$ as the actual distance $d'(t)$ plus a zero-mean random offset δ, and define root mean square (r.m.s.) error in distance measurement to be $\sqrt{\langle \Delta d^2 \rangle}$. Clearly $\langle \Delta d(\Delta t)^2 \rangle$ approaches $2\langle \delta^2 \rangle$ when Δt (and hence $\Delta d'$) becomes small. To find an upper limit on δ, we note that $2\langle \delta^2 \rangle \leq \langle \Delta d(\Delta t_{min})^2 \rangle$ where Δt_{min} is the smallest measured time interval. For the fixed cell data of Figure 2b, $\Delta t_{min} = 12$ sec, and the corresponding $\langle \Delta d(\Delta t_{min})^2 \rangle$ is approximately 0.004 μm^2. We conclude that the r.m.s. distance measurement precision $\sqrt{\langle \Delta d^2 \rangle} \leq 0.04$ μm.

Azide treatment of S. cerevisiae *cells*

Following induction of GFP–LacI, sodium azide was added from a 10% stock solution to give a final concentration of 0.02%. Cells were then incubated in azide for 20 min, then mounted and observed in the continuous presence of azide. Data from 30 cells with an average of 31 time points per data record were combined and plotted in Figure 2b. Growth curves were carried out in the presence and absence of azide and indicated a complete arrest of cell division in the azide-treated cells. The effect of azide on metabolism and active motility is very rapid: addition of 0.02% azide to cells undergoing mitotic division results in an immediate arrest of mitotic chromosome movement; azide addition similarly results in immediate arrest of movements of cortical actin patches in yeast [21].

In vivo *imaging of chromatin motion in* Drosophila

Topoisomerase II injection and imaging were previously described [9]. Three-dimensional images were collected from cycle 12 or 13 embryos, by wide-field deconvolution microscopy [45], using a 60× N.A. 1.4 objective lens and 1.5180 oil. At each time point, a set of 16 256×256 pixel images were collected at focal plane increments of 0.5 μm. One three-dimensional dataset was collected every 20 sec. The nuclear center was defined as the centroid of the nuclear boundary traced from the outline of the nuclear image. The topoisomerase II focus position was defined by interactively picking the spot and taking an intensity-weighted center of mass around the chosen point.

Acknowledgements

The authors thank J. Kilmartin, J. Haber, B. Scalettar, C. Coppin, M. Gustafsson and M. Lowenstein for valuable discussions. We also thank J. Haber, Z. Kam, H. Bass, A. Franklin and members of the Sedat Lab for critical reading of the manuscript. Anti-topoisomerase II antibodies were the kind gift of Neil Osheroff, Vanderbilt University. This work was supported by NIH grants GM-43987 and GM-225101-16 to A.W.M. and J.W.S. respectively. D.A.A. is an investigator of the Howard Hughes Medical Institute. A.W.M. is a David and Lucille Packard Fellow. W.F.M. was supported by a Howard Hughes Medical Institute Predoctoral Fellowship.

References

1. Marshall WF, Fung JC, Sedat JW: Deconstructing the nucleus: global architecture from local interactions. *Curr Opin Genet Dev* 1997, 7:259-263.
2. Abney JR, Cutler B, Fillbach ML, Axelrod D, Scalettar BA: Chromatin dynamics in interphase nuclei and its implications for nuclear structure. *J Cell Biol* 1997, 137:1459-1468.
3. Cremer T, Cremer C, Baumann H, Luedtke CK, Sperling K, Teuber V, Zorn C: Rabl's model of the interphase chromosome arrangement tested in chinese hamster cells by premature chromosome condensation and laser-UV-microbeam experiments. *Hum Genet* 1982, 60:46-56.
4. Parvinen M, Soderstrom KO: Chromosome rotation and formation of synapsis. *Nature* 1976, 260:534-535.
5. De Boni U, Mintz AH: Curvilinear, three-dimensional motion of chromatin domains and nucleoli in neuronal interphase nuclei. *Science* 1986, 234:863-866.
6. Shelby RD, Hahn KM, Sullivan KF: Dynamic elastic behavior of alpha-satellite DNA domains visualized in situ in living human cells. *J Cell Biol* 1996, 135:545-558.
7. Straight AF, Belmont AS, Robinett CC, Murray AW: GFP tagging of budding yeast chromosomes reveals that protein-protein interactions can mediate sister chromatid cohesion. *Curr Biol* 1996, 6:1599-1608.
8. Robinett CC, Straight A, Li G, Willhelm C, Sudlow G, Murray A, Belmont AS: ***In vivo*** localization of DNA sequences and visualization of large-scale chromatin organization using lac operator/repressor recognition. *J Cell Biol* 1996, 135:1685-1700.
9. Swedlow JR, Sedat JW, Agard DA: Multiple chromosomal populations of topoisomerase II detected in vivo by time-lapse, three-dimensional wide-field microscopy. *Cell* 1993, 73:97-108.
10. Gelles J, Schnapp BJ, Sheetz MP: Tracking kinesin-driven movements with nanometre-scale precision. *Nature* 1988, 331:450-453.
11. Qian H, Sheetz MP, Elson EL: Single particle tracking. *Biophys J* 1991, 60:910-921.
12. McClintock B: Cytogenetic studies of maize and neurospora. Carnegie Inst Wash Yearbook 1945, 44:108-112.
13. Maguire MP: The mechanism of meiotic homologue pairing. *J Theor Biol* 1984, 106:605-615.

14. Smithies O, Powers PA: Gene conversions and their relation to homologous chromosome pairing. *Phil Trans Roy Soc Lond Ser B* 1986, 312:291-302.
15. von Smoluchowski, M: Versuch einer mathematischen Theorie der Koagulationskinetik kolloider Loesungen. *Z Phys Chemie* 1917, 92:129-168.
16. Yin H, Wang MD, Svoboda K, Landick R, Block SM, Gelles J: Transcription against an applied force. *Science* 1996, 270:1653-1657.
17. Hirano T, Mitchison TJ, Swedlow JR: The SMC family: from chromosome condensation to dosage compensation. *Curr Opin Cell Biol* 1995, 7:329-336.
18. Koshland D, Strunnikov A: Mitotic chromosome condensation. *Annu Rev Cell Dev Biol* 1996, 12:305-333.
19. Weber V, Harata M, Hauser H, Wintersberger U: The actin-related protein ACT3p of Saccharomyces cerevisiae is located in the nucleus. *Mol Biol Cell* 1995, 6:1263-1270.
20. Milankov K, DeBoni U: Cytochemical localization of actin and myosin aggregates in interphase nuclei in situ. *Exp Cell Res* 1993, 209:189-199.
21. Doyle T, Botstein D: Movement of yeast cortical actin cytoskeleton visualized in vivo. *Proc Natl Acad Sci USA* 1996, 93:3883-3891.
22. Luby-Phelps K, Lanni F, Taylor DL: The submicroscopic properties of cytoplasm as a determinant of cellular function. *Annu Rev Biophys Biophys Chem* 1988, 17:369-396.
23. Heath IB: Behavior of kinetochores during mitosis in the fungus Saprolegnia ferax. *J Cell Biol* 1980, 84:531-546.
24. Mitchison TJ, Sedat J: Localization of antigenic determinants in whole Drosophila embryos. *Dev Biol* 1983, 99:261-264.
25. Dernburg AF, Broman KW, Fung JC, Marshall WF, Philips J, Agard DA, Sedat JW: Perturbation of nuclear architecture by long-distance chromosome interactions. *Cell* 1996, 85:745-759.
26. Hsieh T, Brutlag D: Sequence and sequence variation within the 1.688 g/cm^3 satellite DNA of ***Drosophila melanogaster***. *J Mol Biol* 1979, 135:465-481.
27. Lohe AR, Hilliker AJ, Roberts PA: Mapping simple repeated DNA sequences in heterochromatin of ***Drosophila melanogaster***. *Genetics* 1993, 134:1149-1174.
28. Kas E, Laemmli UK: In vivo topoisomerase II cleavage of the Drosophila histone and satellite III repeats: DNA sequence and structural characteristics. *EMBO J* 1992, 11:705-716.
29. Masumoto H, Masukata H, Muro Y, Nozaki N, Okazaki T: A human centromeric antigen (CENP-B) interacts with a short specific sequence in alphoid DNA, a human centromeric satellite. *J Cell Biol* 1989, 109:1963-1973.
30. Raff JW, Kellum R, Alberts B: The Drosophila GAGA transcription factor is associated with specific regions of heterochromatin throughout the cell cycle. *EMBO J* 1994, 13:5977-5983.
31. Capco DG, Wan KM, Penman S: The nuclear matrix: three-dimensional architecture and protein composition. *Cell* 1982, 29:847-858.
32. Luby-Phelps K, Lanni F, Taylor DL: Behavior of a fluorescent analogue of calmodulin in living 3T3 cells. *J Cell Biol* 1985, 101:1245-1256.
33. Smith DE, Perkins TT, Chu S: Dynamical scaling of DNA diffusion coefficients. *Macromolecules* 1996, 29:1372-1373.
34. Doi M, Edwards SF: *The Theory of Polymer Dynamics.* New York: Oxford University Press;1986.
35. Lang I, Scholz M, Peters R: Molecular mobility and nucleocytoplasmic flux in hepatoma cells. *J Cell Biol* 1986, 102:1183-1190.
36. Fushimi K, Verkman AS: Low viscosity in the aqueous domain of cell cytoplasm measured by picosecond polarization microfluorometry. *J Cell Biol* 1991, 112:719-725.
37. Grosberg AY, Khokhlov AR: *Statistical Physics of Macromolecules.* New York: American Institute of Physics Press; 1994.
38. van den Engh G, Sachs R, Trask BJ: Estimating genomic distance from DNA sequence location in cell nuclei by a random walk model. *Science* 1992, 257:1410-1412.
39. Marshall WF, Dernburg AF, Harmon B, Agard DA, Sedat JW: Specific interactions of chromatin with the nuclear envelope: positional determination within the nucleus in ***Drosophila melanogaster***. *Mol Biol Cell* 1996, 7:825-842.
40. Ogston, AG: The spaces in a uniform random suspension of fibres. *Trans Faraday Soc* 1958, 54:1754-1757.
41. Nicklas RB: Measurements of the force produced by the mitotic spindle in anaphase. *J Cell Biol* 1983, 97:542-548.
42. Khodjakov A, Rieder CL: Kinetochores moving away from their associated pole do not exert a significant pushing force on the chromosome. *J Cell Biol* 1996, 135:315-327.
43. Cremer T, Kurz A, Zirbel R, Dietzel S, Rinke B, Schrock E, *et al.*: Role of chromosome territories in the functional compartmentalization of the cell nucleus. *Cold Spring Harbor Symp Quant Biol* 1993, 58:777-792.
44. Eils R, Dietzel S, Bertin E, Schrock E, Speicher MR, Ried T, *et al.*: Three-dimensional reconstruction of painted human interphase chromosomes: active and inactive X chromosome territories have similar volumes but differ in shape and surface structure. *J Cell Biol* 1996, 135:11427-11440.
45. Agard DA, Hiraoka Y, Shaw P, Sedat JW: Fluorescence microscopy in three dimensions. *Methods Cell Biol* 1989, 30:353-377.
46. Lee GM, Ishihara A, Jacobson KA: Direct observation of Brownian motion of lipids in a membrane. *Proc Natl Acad Sci USA* 1991, 88:6274-6278.

Because *Current Biology* operates a 'Continuous Publication System' for Research Papers, this paper has been published on the internet before being printed. The paper can be accessed from http://biomednet.com/cbiology/cub – for further information, see the explanation on the contents page.